Provided for non-commercial research and educational use only.
Not for reproduction or distribution or commercial use.

This article was originally published by IWA Publishing. IWA Publishing recognizes the retention of the right by the author(s) to photocopy or make single electronic copies of the paper for their own personal use, including for their own classroom use, or the personal use of colleagues, provided the copies are not offered for sale and are not distributed in a systematic way outside of their employing institution.

Please note that you are not permitted to post the IWA Publishing PDF version of your paper on your own website or your institution's website or repository.

Please direct any queries regarding use or permissions to wqrjc@iwap.co.uk

Experimental assessment of Athabasca River cohesive sediment deposition dynamics

Juan Garcia-Aragon, Ian G. Droppo, Bommanna Krishnappan, Brian Trapp and Christina Jaskot

ABSTRACT

Polycyclic aromatic hydrocarbons (PAHs) originating from natural sources, and potentially from the Athabasca Oil Sands development, are of concern for the Athabasca River and Lake Athabasca delta ecosystems. In order to model the transport of fine sediments (and associated PAHs), it is important to describe the sediment dynamics within the river system. Flocs possess different settling characteristics compared to individual particles. A key aspect in modelling floc settling behaviour is the mathematical linkage of the floc density to floc size. In this paper, a rotating annular flume is used to determine the settling characteristics of Muskeg River (a tributary of the Athabasca River) sediments under different shear conditions. Simulations of the settling and flocculation behaviour of these sediments were used to calibrate a density vs. floc size model. A relationship of the parameters relating floc size and density with the fractal dimension *F* shows that as diameter increases flocs become weaker. Recommendations for the practical application of the model are further formulated in this paper. The deposition tests offer a quantitative measure of the relative amount of sediment that is likely to be transported through the river for given flow conditions.

Key words | cohesive sediments, floc density, floc porosity, rotating annular flume, settling velocity

Juan Garcia-Aragon
Facultad de Ingeniería,
Centro Interamericano de Recursos del Agua,
FI-UAEM,
Cerro de Coatepec s/n,
Ciudad Universitaria,
C.P. 50130,
Toluca,
Estado de México,
México

Ian G. Droppo (corresponding author)
Bommanna Krishnappan
Brian Trapp
Christina Jaskot
NWRI,
Environment Canada,
867 Lakeshore Road,
Burlington, ON, L7R 4A6,
Canada
E-mail: *ian.droppo@ec.gc.ca*

INTRODUCTION

The Athabasca River drains an area of approximately 138,000 km^2 and flows nearly 1,400 km from its headwaters in the Glacier National Park to the Peace–Athabasca Delta and Lake Athabasca. The Athabasca River system includes a total of 94 rivers, over 150 named creeks, numerous unnamed creeks and 153 lakes (Kellerhals *et al*. 1972). Large oil sands developments are located in the Athabasca River basin and there are concerns about hydrocarbon pollution in the lower reaches below Fort McMurray (Headley *et al*. 2001) (Figure 1). Flowing north from Fort McMurray, the Athabasca River is joined by several smaller tributaries, including the Steepbank, Muskeg and Firebag rivers flowing from the east and the MacKay and Ells rivers from the west. Industrial development has occurred within many of these catchments that have the potential to physically alter the landscapes affecting drainage patterns and groundwater–surface water interactions and through industrial water extraction and discharge. The Muskeg River basin is one such catchment that is undergoing rapid change. According to Alberta Environment (2008) in the Muskeg River basin, there are two ongoing oil sands operators covering an area of 122.7 km^2 (8% of basin area); there are six additional projects approved covering 454.1 km^2 (31% of the area) and two more planned covering 138 km^2 (9.3% of the basin area). In the not too distant future, almost half of the basin area will be disturbed by oil sands development.

The mobilisation, transport and fate of polycyclic aromatic hydrocarbons (PAHs) is primarily controlled by the sediment dynamics within the river basin as these hydrophobic compounds favour adsorption to high surface area to volume cohesive sediment particles. As it is well known

doi: 10.2166/wqrjc.2011.030

Figure 1 | Location of sample site on the Muskeg River at the confluence of the Athabasca River.

that cohesive sediments will flocculate together to form larger particles (flocs) and that these are generally the dominant form of sediment transported in suspension (Droppo 2001; Jarvis *et al.* 2005), the structure of the floc will play a large role in the dynamics of the sediment within the system. Flocs are composed of an active biological component (primarily bacteria, although at times other organisms can be incorporated), a nonviable biological component (e.g. detritus, extracellular polymeric substances (EPS)), inorganic particles (e.g. clay particles) and water held within or flowing through pores (Droppo 2001; Williams *et al.* 2008). The effect of flocculation is to increase the downward flux of sediment within the system. The relative magnitude of this flux is controlled primarily by floc size, porosity and density. Of these three factors, the dominant one will often be size; however density, which is autocorrelated to porosity, can also influence the settling velocity of the flocs and therefore associated PAHs (Droppo 2004). As flocs increase in size their density decreases due to an increase in porosity with a resultant drop in settling velocity. Density can have a significant influence on floc settling, only if there is a large range in density with floc size. Often the range in floc density over a sample population can be small and close to that of water (Droppo *et al.* 2005).

The majority of models formulated to define the relationship between floc density and floc size are valid for limited experimental conditions (Zahid & Ganczarczyk 1990; Andreadakis 1993). For example, Andreadakis (1993) proposed the following equation for the floc density (ρ_s) for a dried sludge with a density of 1,340 kg/m^3:

$$\rho_s = 1 + 0.3D^{-0.82} \tag{1}$$

where D is the floc diameter.

Zahid & Ganczarczyk (1990) proposed Equation (2) for a kaolin–polymer aggregate of a perfect sphere:

$$\rho_s = 1.05D^{(-0.0038\mathrm{pH}+0.00716)} \tag{2}$$

Gregory (1997) states that buoyant floc density plotted against floc size presents a relationship of the form

$$\rho_s = BD^{-C} \tag{3}$$

where B and C are constants and the exponent C is related to the fractal dimension F ($F = 3–C$). The value of C was shown experimentally to vary between 1 and 1.4, which corresponds to F values between 2 and 1.6, reducing the uncertainty in the definition of F. The lower the value of F the less compact is the floc.

Other authors have also tried to extend the validity of these models based on fractal dimensions (Khelifa & Hill 2006; Son & Hsu 2009) by varying the fractal dimension (F) as a function of floc size. For example, an equation proposed by Khelifa & Hill (2006) (an extension of the Kranenburg (1994) model) is

$$\rho_s - \rho = (\rho_p - \rho)\left(\frac{D}{D_{50}}\right)^{F-3} \tag{4}$$

where D_{50} is the median diameter of the mixture and ρ_p is the density of the parent material.

They found that F is a function of particle diameter. This research also shows that F is a function of shear rate. Hoekstra *et al.* (1992) have reported that for orthokinetic aggregation (in Couette flow) at high salt concentration

the fractal dimension is shear-dependent, increasing from 1.7 at zero shear rate to about 2.2 at a shear rate of 200 s^{-1}.

In order to develop models of pollutant transport in the Athabasca River, the transport behaviour of flocculated sediment needs to be defined in relation to the structural properties that influence their dynamics within the river. The objective of this paper is to investigate, using an annular flume and a numerical model, the density vs. size relationship as it pertains to the deposition process of the fine-grained sediment. Integration of the floc deposition process into models will enable water resource managers to predict the fate of potentially pollution-laden cohesive sediments.

METHODS

Sediment sample collection and preparation

Recently deposited bed sediment samples were collected from the Muskeg River at the confluence of the Athabasca River on October 6 and 7, 2009 using an inverted cone sampler (Krishnappan 2007). The sampler consists of a conical chamber fitted with a propeller and a submerged pump. While wading, the sampler was manually lowered to the bed where a propeller generated enough turbulence for the submersible pump to pump water and resuspended sediment to 100 L polyethylene containers located in the back of a pickup truck. In all, 800 L of water and sediment were collected, with the sampler moved multiple times in a small area. The containers were shipped from Fort McMurray, Alberta to Environment Canada in Burlington, Ontario, in a refrigerated truck to support the annular flume experiments.

Deposition experiments

The deposition characteristics of fine sediments from the Muskeg River were studied in a rotating annular flume at the National Water Research Institute – Environment Canada, Burlington, Ontario. The flume consists of a circular channel, which is 5.0 m in diameter, 0.30 m in width and 0.30 m in depth (Figure 2). This channel rotates in one direction while a top cover that fits inside the flume and just touches the water surface rotates in the opposite direction. This counter-rotation helps to generate a two-dimensional turbulent shear flow with nearly constant bed-shear stress across the width of the channel (Petersen & Krishnappan 1994). A full description of the flume can be found in Krishnappan (1993).

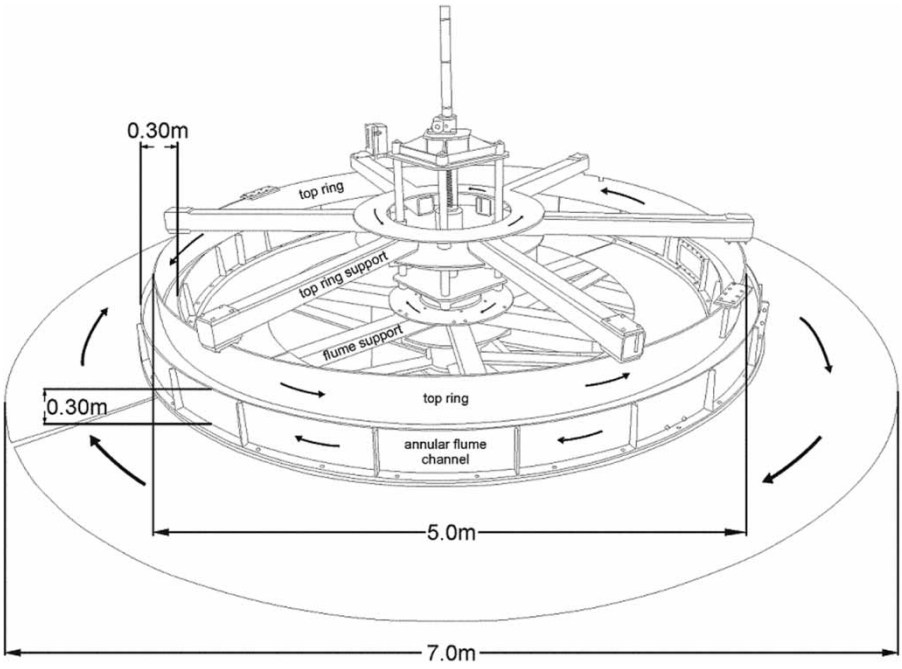

Figure 2 | Schematic of 5 m annular flume.

The flume was interfaced with a CILAS™ 930 laser particle size analyser to generate real-time particle size distributions during flume operation (a distribution was created every 7 min over the duration of an experimental run). The instrument operates on the principle of laser diffraction and is operated in a continuous flow-through mode generating distributions within the range of 0.2–500 μm in size.

The sediment–water samples were stored in a cold room at 4 °C prior to testing at which point the samples were allowed to equilibrate to room temperature. The sediment–water mixture of the Muskeg River was placed in the flume at a concentration of approximately 325 mg/L. The initial concentration was chosen to represent a realistic concentration for the Athabasca River downstream from Fort McMurray (mean for Athabasca River is 400 mg/L). The sediment–water mixture was then thoroughly mixed, first with a mechanical mixer and then by running the flume at a high shear level of 0.461 Pa. After operating the flume at this high speed for 20 min, the shear within the flume was lowered to predetermined levels (0.058, 0.121, 0.165 and 0.265 Pa) to provide a range of bed-shear stresses for the assessment of particle deposition dynamics. Suspended sediment (SS) samples were withdrawn from the flume through a sampling port located at the mid-depth at 5 min intervals during the first hour of the test and every 10 min thereafter until the completion of the test. A test was considered complete when the SS concentration remained nearly constant for about an hour. This took about 5 h in most tests. A plankton chamber sample was also collected at the end of each experiment for gross morphological characterisation of the flocs remaining in suspension using image analysis following the techniques described by Droppo *et al.* (1997). Sediment–water samples were analysed for the concentration of SS by a gravimetric method, which consisted of filtering the sample on Millipore™ 0.45 μm filters, and drying for 1 h at 100 °C and weighing the residue.

Numerical model simulation

The numerical model developed by Krishnappan & Marsalek (2002) was used to describe the behaviour of sediment particles, in which their motion is considered in two stages: (1) a settling stage and (2) a flocculation stage. These stages were assumed to occur alternately during each time step of modelling. The settling stage is analysed using a one-dimensional unsteady advection–diffusion equation:

$$\frac{\partial C_k}{\partial t} + w_k \frac{\partial C_k}{\partial z} = \frac{\partial}{\partial z}\left(\zeta \frac{\partial C_k}{\partial z}\right) \tag{5}$$

where C_k is the volumetric concentration of sediment of the kth size fraction and w_k is the fall velocity of that fraction, ζ is the turbulent diffusion coefficient, t is the time and z is the vertical distance from the water surface. Equation (5) expresses the balance between the settling flux ($w_k C_k$) and the diffusive flux $\zeta(\partial C_k/\partial z)$ in the vertical direction. To solve this equation, boundary conditions at the water surface and the bed have to be specified along with an initial condition expressing the sediment concentration as a function of the vertical distance at time $t = 0$. At the water surface (top boundary), it is assumed that there is no net transfer of sediment across this boundary and therefore the settling flux is equal to the diffusive flux. At the bottom boundary, the net upward flux of sediment is equated to the difference between the erosion flux and the deposition flux.

The flocculation stage of the settling process was described by a coagulation equation according to the model developed by Krishnappan & Marsalek (2002), which expresses the number–concentration balance of particles undergoing coagulation as a result of the collision of particles of different size classes. The most sensitive parameter for the flocculation model is the floc density. A relationship between the density of the floc and the diameter is needed. In this work we used the following relationship for the floc density (ρ_s) as proposed by Lau & Krishnappan (1997):

$$\rho_s - \rho = (\rho_p - \rho)\exp(-bD^c) \tag{6}$$

where ρ and ρ_p are the densities of water and parent material forming the floc in kg/m^3, D is in microns, and b and c are empirical coefficients. These coefficients are dependent on the type of sediment and, as will be discussed later, also depend on the shear stress applied.

Using Equation (6) and the Stokes equation, the following relationship for the settling velocity is obtained:

$$w_k = \frac{0.545(\rho_p/\rho - 1)D_{1k}^2}{\nu}\exp(-bD_{2k}^c) \quad (7)$$

where ν is the kinematic viscosity of water, D_{1k} and D_{2k} are the mean floc diameter of the kth fraction expressed respectively in m and in microns.

In this paper we extend the application of Equation (6) to Muskeg River sediments with parameters b and c defined through the calibration of the model with the experimental results in order to assist in the determination of sediment and PAH fate within the Athabasca River system.

RESULTS AND DISCUSSION

Experimental interpretation

Flocs remaining in suspension were typically irregular in shape with high porosity and water content (Figure 3). While no higher resolution microscopy was performed for our deposition experiments, subsequent erosion experiments of the same sediment (Garcia-Aragon *et al.* 2011) were assessed with confocal scanning laser microscopy and transmission electron microscopy. This imaging illustrated the prevalence of the microbial community and their production of EPS, forming a structural network of pores within the flocs with significant capacity to retain water and reduce floc density.

Figure 4 illustrates the SS concentration in the water column as a function of time for four different bed-shear stresses during deposition experiments. For all runs, the SS concentration initially decreases rapidly followed by an SS concentration that approaches a steady state (equilibrium). For example, for the lowest bed-shear stress tested (0.058 Pa), the SS concentration after 6 h of settling was approximately 30 mg L^{-1} (8% of the initial concentration) and still declining, whereas for the highest shear stress (0.265 Pa), the steady state SS concentration was approximately 160 mg L^{-1} (53% of the initial concentration). For a bed-shear stress of 0.058 Pa, the majority of SS is likely to be deposited given its continued settling. As such, the critical shear stress for sediment deposition of Muskeg River sediments is slightly higher than 0.058 Pa and lower than 0.121 Pa.

The deposition tests also offer a quantitative measure of the amount of sediment that is likely to be transported through the river for given flow conditions. For example, if the flow conditions in the river are such that the bed-shear stress is less than the critical shear stress for deposition, all of the SS and associated PAHs entering the river would be deposited within the Muskeg River and not be delivered to the Athabasca River. On the other hand, if the bed-shear stress is around 0.265 Pa, then about 50% of the suspended

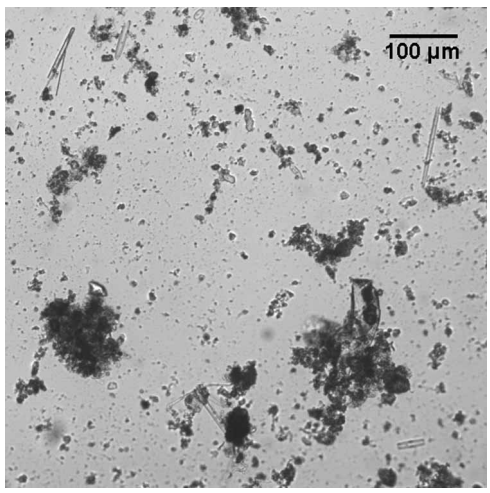

Figure 3 | Representative suspended Muskeg River flocs sampled 5 min after the flume shear was reduced from 0.461 to 0.165 Pa. Flocs are irregular in shape with high porosity and water content.

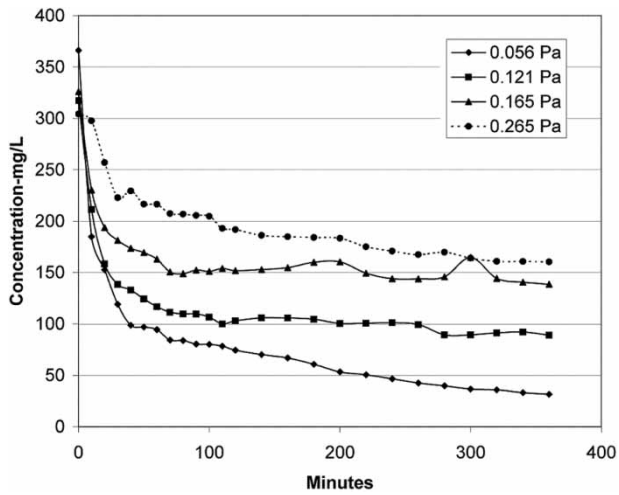

Figure 4 | Change in SS concentration with time for four different shear levels.

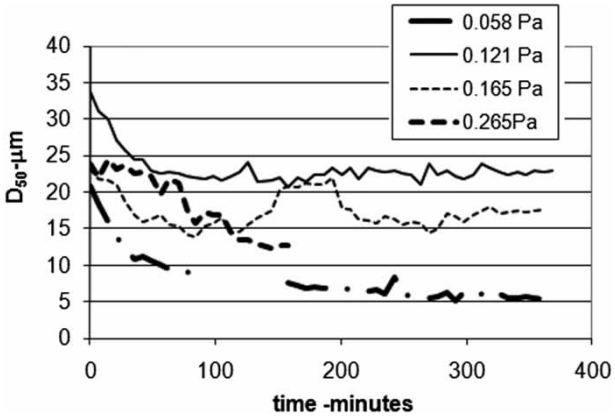

Figure 5 | Change in median floc size (D_{50}) with time for four different shear levels.

material and any associated PAHs would be transported into the Athabasca River. Knowing the flow velocity field and the spatial and temporal variation of the bed-shear stress, the results from the deposition tests can be used to make quantitative estimates of sediment deposition and transport in river systems.

Sediment dynamics within the Muskeg River can also be inferred when assessing changes in SS particle size. Figure 5 demonstrates some interesting floc-size-carrying capacity differences, likely influenced by flocculation and floc breakage with changes in time and shear levels. In all cases, with the exception of the highest shear (0.265 Pa), the D_{50} values dropped initially followed by an equilibrium particle size supported by the flow condition. The extent and rate of floc size reduction in suspension, during the first 2 h, was greatest for the two lowest shears (0.058 and 0.121 Pa), which is indicative of larger flocs settling out of suspension. This is particularly the case for the lowest shear as seen in Figure 6(a) where there is a substantial shift in the grain size distribution to smaller sizes. At this low shear level, it is very likely that active flocculation is continuing throughout the experimental run, resulting in the slow removal of particles. This is evident by the very gradual decline in the slope to a D_{50} value to approximately 5 µm and the continued reduction in SS concentration (Figure 4). The next higher shear stress (0.121 Pa) resulted in the largest particle size (D_{50}) being kept in suspension after an initial drop of 15 µm one hour into the run. This indicates that, at this turbulence level, flocs are kept in

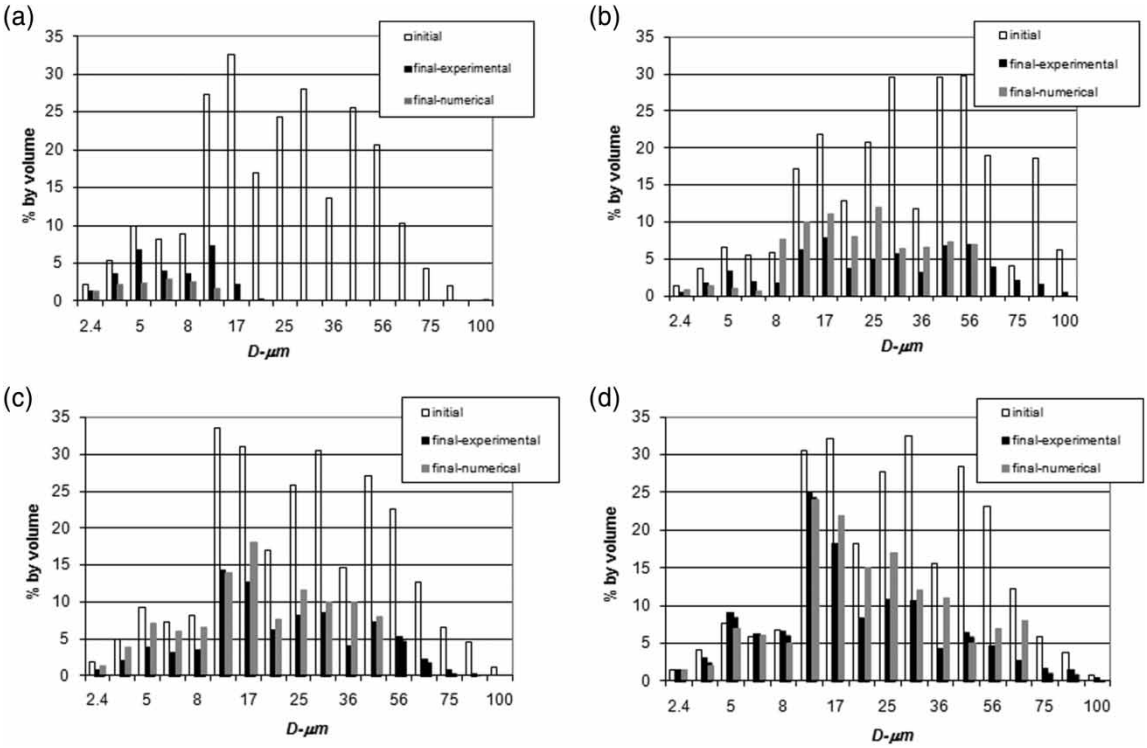

Figure 6 | Change in grain size distributions from initial distribution (prior to change in shear) and at the end of each shear level. (a) 0.058 Pa, (b) 0.121 Pa, (c) 0.165 Pa and (d) 0.265 Pa. The numerical predictions of grain size are also presented.

suspension but the shear is not enough to break up the flocs. Figure 6(b) shows that, while there is loss of sediment due to deposition, there is still a representative amount of sediment in each of the original size classes. This is also substantiated by the SS concentration remaining relatively consistent after the initial settling out of sediment (Figure 4). For a shear level of 0.165 Pa, there is a further drop in D_{50} (although variation was high for this run due to clogging of the CILAS™ 930 cell). Nevertheless an equilibrium particle size was attained quickly. Although the SS concentration remaining in suspension increased at this shear level (Figure 4), the reduction in particle size in suspension at equilibrium (Figure 6(c)) suggests that there has been some floc breakage occurring. At a shear of 0.265 Pa, the floc size continued to decrease without reaching an equilibrium, suggesting that there is further floc breakage at this shear (although the length of record for this shear is lower – 160 min). Figure 6(d) shows this apparent floc breakage by the increase in the volume of particles at the smaller size classes for the higher shears. Theory would suggest that an equilibrium condition would eventually prevail for both size and concentration for this shear level. An anomaly in this dataset is that the SS concentration did continue to drop over the duration of this shear level. This may be an artefact of some edge effects and is not believed to be due to flocculation at this high shear.

Modeling interpretation

Figure 7 and Table 1 summarises the numerical simulation in relation to the measured experimental results and

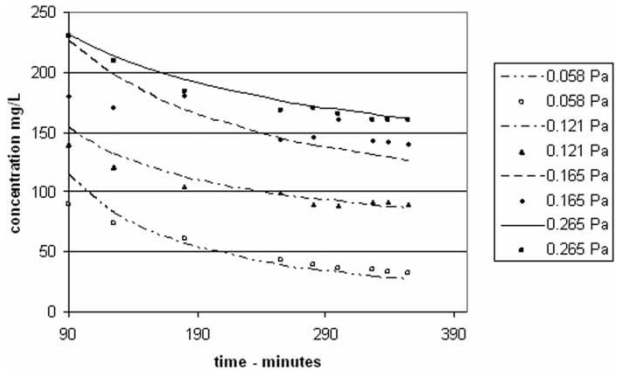

Figure 7 | Comparison between simulation and experimental results after 90 min of settling for four different shear levels.

Table 1 | Experimental and numerical simulation results with varying *b* and *c*

Shear stress (Pa)	Numerical final concentration (mg/L)	Experimental final concentration (mg/L)	*b*	*c*
0.058	30	35	0.02	1.35
0.121	90	91	0.02	1.45
0.165	130	142	0.03	1.45
0.265	160	160	0.03	1.55

demonstrate reasonable fits between the two (poorest fit for the shear stress of 0.165 Pa). Figure 7 and the numerical modelling are not shown for the first hour of the simulations due to the initial sharp drop in SS, making differentiation difficult between runs. The modelling results were used to assess the change in concentration and particle size during periods when the system was at or near equilibrium. In order to achieve the reasonable prediction of the final equilibrium concentration in Figure 7, the coefficients of *b* and *c* had to be adjusted. This is contrary to previous flocculation models which have consistent coefficients regardless of shear level (Krishnappan & Marsalek 2002). It is hypothesised, and discussed further below, that the values of both *b* and *c* are controlled by the shear level influencing floc structure (size, density, porosity) and therefore floc hydrodynamic behaviour (i.e. settling, collision frequency).

As density is highly correlated to many floc structural properties such as size (density decreases when floc size increases) and porosity (density decreases when porosity increases), and can influence hydrodynamic behaviour such as settling (Droppo 2004; Gerbersdof *et al.* 2007; Son & Hsu 2009), Equation (6) was applied for a range of floc sizes and for each shear stress level with associated *b* and *c* coefficients listed in Table 1 (Figure 8). The general trends presented in Figure 8 (i.e. density decreases and approaches that of water with increasing floc size), regardless of shear level, are consistent with trends observed by others (Khelifa & Hill 2006) and are related to the increase in void space as flocs grow, resulting in a higher bound water content and thus a lower density. Although there are differences in the predicted densities with shear (Figure 8), all of the plots converge to have similar density at floc sizes above 50 μm (close to 1.0 gm cm^{-3}). This would suggest that, for the modelled shear values assessed, settling

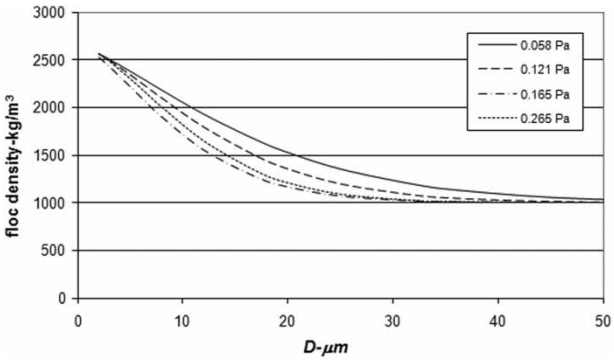

Figure 8 | Results of applying Equation (5) based on particle size and the coefficients of *b* and *c* as defined in Table 1 for each shear level.

velocity of flocs larger than 50 μm are predicted not to be influenced by density as they are essentially equal to that of water. It follows then that, although shear-dependent, floc size is the dominant factor controlling floc settling when flocs grow to be large (Droppo 2004). In a separate analysis Garcia-Aragon *et al.* (2011), found that Muskeg River flocs settled in quiescent conditions (ranging in size from 100–450 μm in diameter) had densities ranging from 1,000–1,300 kg/m^3. It should be realised that floc size is highly influenced by shear and, if higher shear values were applied than used in these experiments and models, it would be expected that the density would increase as flocs are broken up into smaller particles/flocs.

While the model predicts that shear is independent of floc density (assuming no floc breakage) for particles greater than 50 μm, it does predict that there is some effect of shear on floc density for flocs less than 50 μm. Using the 20 μm size as an example, density decreases with increasing shear from 0.058 to 0.165 Pa (a drop of approximately 500 kg/m^3) but increases when the shear is further increased to 0.265 Pa. This numerical relationship seems to be borne out for the lower shear values (0.058–0.121 Pa) where the concentration and particle size data provided above suggest that flocculation is occurring. That is, flocculation is believed to be actively occurring at 0.121 Pa whereas at 0.058 Pa there is rapid deposition with a loss of sediment from suspension (in fact, at the end of the 0.058 Pa run there are only particles below 17 μm remaining in suspension; at the end of the 0.121 Pa run there are particles as large as 85 μm still in suspension). As such, a 20 μm particle remaining in suspension following a reduction in shear from 0.461 to 0.058 Pa will be structurally more compact with lower porosity and higher density than the 20 μm floc formed by flocculation at 0.121 Pa (Figure 8).

This trend is shown in the numerical simulation by the decrease in F (a measure of floc compaction). Lower values of F indicate less compact flocs. The F in the experiments can be calculated with Equation (8) deduced from a comparison between the Khelifa & Hill (2006) model (Equation (4)) and Equation (6) used in this research. The following relationship between F and the parameters b and c is obtained:

$$F = 3 - \frac{(-bD^c)}{\ln(D/D_{50})}. \quad (8)$$

Using the experimental values of b and c and the average particle size in each experiment (each shear rate), Figure 9 is obtained. This figure clearly shows a decrease in fractal dimension F as D increases for different shear rates. Thus the experimental decrease in F in this research with particle size indicates that flocs are less compact as diameter increases for all shear stresses. This decrease in floc compaction as D increases helps explain the settling behaviour of flocs for the different shear stresses shown in Figure 10.

The model used for the settling velocity in this paper (Equation (7)) shows the effect of shear stress on settling velocity and that for particles larger than 50 μm settling velocity is almost zero for high shears (Figure 10). This fact helps explain the steady state concentration shown in Figure 4. Otherwise, if settling velocity continues to grow with size this equilibrium concentration would have never

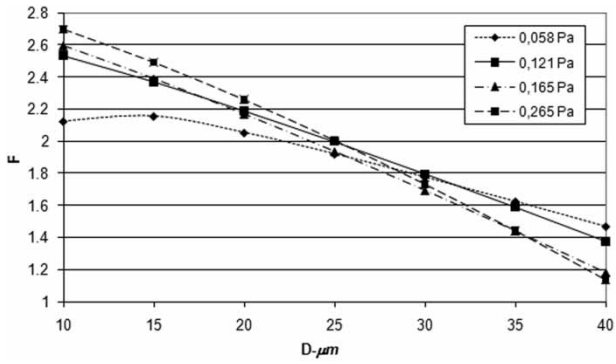

Figure 9 | Relationship between *F* and floc size for different shear rates.

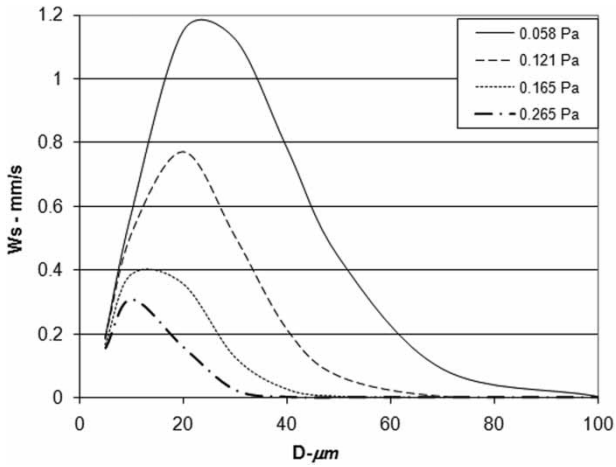

Figure 10 | Variation of settling velocity with shear stress according to numerical simulation.

been reached. Many models in the literature relating floc size to settling velocity show a continuous increase in settling velocity with increase in floc size (Khelifa & Hill 2006). These models do not take into account the effect of hydrodynamics on settling velocity and of shear stress on the density of flocs. Further research is needed to extend the application of Equation (6) for higher floc sizes and shear stresses.

CONCLUSIONS

Depositional experiments within a rotating annular flume using cohesive sediments from the Muskeg River, a tributary of the Athabasca River, Alberta, Canada, suggest that fluid shear may influence the structural characteristics of the flocs which, in turn, may influence sediment and associated contaminant deposition dynamics within the system. Visual observations of flocs during deposition at all shears showed floc structures with an open matrix and high water content. Measured floc density over an array of representative floc sizes, however, showed a low range in density from 1,001–1,300 kg m^{-3}. Therefore, a small change in floc density will not influence settling to a great extent. However, it is clear that the low density (close to that of water) will result in the particles remaining in suspension, as predicted by the model and laboratory results, particularly those greater than 50 μm at higher shears. Differences in floc density with shear were found for smaller particles (<50 μm) which were shown (decrease in F with increase in D) to be due to differences in floc structure resulting from different shear forces. This conclusion was supported by the need to change the coefficients (b and c) within the density prediction equation for adequate identification of suspended solids concentrations remaining in suspension at equilibrium. It is concluded that, while shear dictates the proportion of sediments remaining in suspension vs. that deposited, it can also influence floc strength and structure (with some density effects), but that these changes have a larger impact on small floc settling behaviour. This work will assist in the prediction of the fate of pollutants (including PAHs) in the Athabasca River watershed, with values of b and c in Equation (6) being defined according to the particle size distribution and mean shear stress. The experimental results show that, if the Muskeg River bed-shear stress is around 0.265 Pa, then about 50% of the suspended material and any associated PAHs would be transported into the Athabasca River. Therefore results from the deposition tests can be used to make quantitative estimates of sediment deposition and transport in the river system.

ACKNOWLEDGEMENT

The first author would like to thank the CONACYT Mexican funding agency for the economic support during his sabbatical leave at NWRI.

REFERENCES

Alberta Environment 2008 Muskeg River Interim *Management Framework for Water Quantity and Quality Summary Report*. Alberta Environment Information Centre, Edmonton, Alberta, Canada. ISBN: 978-0-7785-7631-0.

Andreadakis, A. C. 1993 Physical and chemical properties of activated sludge flocs. *Wat. Res.* **27** (12), 1707–1714.

Droppo, I. G. 2001 Rethinking what constitutes suspended sediment. *Hydrol. Process.* **15**, 1551–1564.

Droppo, I. G. 2004 Structural controls on floc strength and transport. *Can. J. Civil Engng.* **31**, 569–578.

Droppo, I. G., Leppard, G. G., Flannigan, D. T. & Liss, S. N. 1997 The fresh water floc a functional relationship of water and organic and inorganic floc constituents affecting suspended sediment properties. *Wat. Air Soil Pollut.* **99**, 43–53.

Droppo, I. G., Leppard, G., Liss, S. & Milligan, T. 2005 *Flocculation in Natural and Engineered Environmental Systems*. CRC Press, Boca Raton, FL.

Garcia-Aragon, J., Droppo, I. G., Krishnappan, B. G., Trapp, B. & Jaskot, C. 2011 Erosion characteristics and floc strength of Athabasca River cohesive sediments: towards managing sediment related issues. *J. Soils Sediments* **11**, 679–689.

Gerbersdof, S. U., Jancke, T. & Westrich, B. 2007 Sediment properties for assessing the erosion risk of contaminated riverine sites. *J. Soil Sediments* **7**, 25–35.

Gregory, J. 1997 The density of particle aggregates. *Wat. Sci. Technol.* **36** (4), 1–13.

Headley, J. V., Akre, C., Conly, F. M., Peru, K. M. & Dickson, L. C. 2001 Preliminary characterization and source assessment of PAHs in tributary sediments of the Athabasca River, Canada. *Environ. Forensis* **2**, 335–345.

Hoekstra, L. L., Vreeker, R. & Agterhof, W. G. M. 1992 Aggregation of nickel hydroxycarbonate studied by light scattering. *J. Colloid Interface Sci.* **151**, 17–25.

Jarvis, P., Jefferson, B., Gregory, J. & Parsons, S. A. 2005 A review of floc strength and breakage. *Wat. Res.* **39**, 3121–3137.

Kellerhals, R., Neill, C. R. & Bray, D. I. 1972 *Hydraulic and Geomorphic Characteristics of Rivers in Alberta*. Alberta Cooperative Research Program in Highway and River Engineering; Research Council of Alberta River Engineering and Surface Hydrology report 72-1. Edmonton, Alberta.

Khelifa, A. & Hill, P. S. 2006 Models for effective density and settling velocity of flocs. *J. Hydraul. Res.* **44** (3), 390–401.

Kranenburg, C. 1994 The fractal structure of cohesive sediment aggregates. *Estuarine Coastal Shelf Sci.* **39**, 451–460.

Krishnappan, B. G. 1993 Rotating circular flume. *J. Hydraul. Engng.* **119** (6), 758–767.

Krishnappan, B. G. 2007 Recent advances in basic and applied research in cohesive sediment transport in aquatic systems. *Can. J. Civil Engng.* **34**, 731–743.

Krishnappan, B. G. & Marsalek, J. 2002 Modelling of flocculation and transport of cohesive sediment from an on-stream stormwater detention pond. *Wat. Res.* **36**, 3849–3859.

Lau, Y. L. & Krishnappan, B. G. 1997 *Measurement of Size Distribution of Settling Flocs*. NWRI Publication no. 97-223. National Water Research Institute, Environment Canada, CCIW, Burlington, ON, Canada.

Petersen, O. & Krishnappan, B. G. 1994 Measurement and analysis of flow characteristics in a rotating circular flume. *J. Hydraul. Res.* **32** (4), 483–494.

Son, M. & Hsu, T. J. 2009 The effect of variable yield strength and variable fractal dimension on flocculation of cohesive sediment. *Wat. Res.* **43**, 3582–3592.

Williams, N. D., Walling, D. E. & Leeks, G. J. L. 2008 An analysis of the factors contributing to the settling potential of fine fluvial sediment. *Hydrol. Process.* **22**, 4153–4162.

Zahid, W. M. & Ganczarczyk, J. J. 1990 Suspended solids in biological filter effluents. *Wat. Res.* **27**, 215–220.

First received 21 October 2010; accepted in revised form 13 June 2011